

# Magnetic field profile generation software

A. LABICHE, J. TAQUIN

U2R2M, Université de Paris-Sud, 91405 Orsay (FRANCE)

## I. ABSTRACT

Good precision magnetic field is often required for magnetic resonance imaging experiments. One of the possibilities to create such field is to use Legendre expansion of the Green function. We propose a method to correct field defects over the volume of interest by means of a series of small permanent magnetic rods (shims) the position of which is determined by a computer software. This method also can be used to create almost any field with negligible high-order harmonics above a fixed value.

## II. INTRODUCTION

The Legendre expansion to calculate magnetic source positions proposed by [1] and [5] serves as our generic function. However, for simplicity of realization, we use only a minimum of generators. The first part of the problem is to choose an initial configuration which is capable of physically creating any required field intensity. Experience shows that a lot of initial designs cannot be used. We propose only those who satisfy the design conditions. The final corrected field has an improved homogeneity of the order of 2 to 3 (ratio of 100 to 1000).

## III. MATHEMATICAL METHOD

The spherical co-ordinate system is the most convenient to use because one can easily express the field profile with three dimensional Taylor series (derivation at the origin), thereafter pass on directly to the Legendre coefficients [3, p.1274]. The z-axis field induction  $B_z$  generated by a magnet with only a z magnetization  $M_z$  is given by:

$$B_z = \frac{M_z}{4\pi} \int_S \left[ \frac{\partial}{\partial z} \frac{1}{R} \right]_{z_1}^{z_2} dx' dy' \quad (1)$$

where  $R = \|\vec{x} - \vec{x}'\|$  is the distance between the source  $\vec{x}'$  and the calculated point  $\vec{x}$  and  $S$  is the cross section of the magnet.

$$\frac{\partial}{\partial z} \frac{1}{R} = - \sum_{n=0}^{\infty} \sum_{m=0}^m \epsilon_m \frac{(n-m+1)!}{(n+m)!} P_{nm}(\cos \theta) P_{n+1m}(\cos \theta') \cdot \frac{r^n}{r'^{n+2}} \cos [m(\phi - \phi')] \quad (2)$$

where  $P_{nm}$  are the associated Legendre polynomials and  $\epsilon_m = 1$  if  $m = 0$  and 2 if  $m > 0$ .

It is very difficult to integrate Eq.(1) along  $x'$  and  $y'$ . We replace this integration by the cross section  $A$ , so the error should be important if the calculated point is close to the source.

We obtain from Eq.(1) and Eq.(2)

$$B_z(\rho, \theta, \phi) = -\frac{M_z A}{4\pi} \sum_{n=0}^{n=\infty} \sum_{m=0}^{m=n} \epsilon_m \frac{(n-m+1)!}{(n+m)!} \left[ \frac{P_{n+1m}(\cos \theta')}{r'^{n+2}} \right]_{z_1}^{z_2} \cdot r^n P_{nm}(\cos \theta) \cos [m(\phi - \phi')] \quad (3)$$

If  $A_{nm}$  and  $B_{nm}$  are the coefficients of the decomposition of measured field, summed to the total magnetic field produced by the N magnets,

$$\begin{aligned} & \frac{1}{4\pi} \sum_{n=0}^{N_{ordres}} \sum_{m=0}^n (A_{nm} \cos(m\phi) + B_{nm} \sin(m\phi)) r_{mes}^n P_{nm}(\cos \theta) + \\ & - \frac{M_z A}{4\pi} \sum_{n=0}^{N_{ordre}} \sum_{m=0}^{m=n} \epsilon_m \frac{(n-m+1)!}{(n+m)!} \left[ \frac{P_{n+1m}(\cos \theta')}{r'^{n+2}} \right]_{z_1}^{z_2} \cdot \\ & r^n P_{nm}(\cos \theta) [\cos(m\phi) \cos(m\phi') + \sin(m\phi) \sin(m\phi')] = 0 \end{aligned} \quad (4)$$

In order to respect the orthogonality property of Legendre expansion, the only solution of Eq.(4) is to annul each term of the serie. We obtain the following system

$$\left\{ \begin{array}{l} \underbrace{\frac{A_{nm}}{4\pi} - \sum_{i=1}^N \frac{M_i A_i}{4\pi} \epsilon_m \frac{(n-m+1)!}{(n+m)!} \left[ \frac{P_{n+1m}(\cos \theta'_i)}{r_i'^{n+2}} \right]_{z_{i1}}^{z_{i2}} \cos(m\phi'_i)}_{=} = 0 \\ \underbrace{\frac{B_{nm}}{4\pi} - \sum_{i=1}^N \frac{M_i A_i}{4\pi} \epsilon_m \frac{(n-m+1)!}{(n+m)!} \left[ \frac{P_{n+1m}(\cos \theta'_i)}{r_i'^{n+2}} \right]_{z_{i1}}^{z_{i2}} \sin(m\phi'_i)}_{=} = 0 \end{array} \right. \quad (5)$$

We can use the minus letters  $a_{nm}$ ,  $b_{nm}$  to represent the quantity shown by the underbrackets

$$\left\{ \begin{array}{l} \frac{A_{nm}}{4\pi} - \frac{a_{nm}}{4\pi} = 0 \\ \frac{B_{nm}}{4\pi} - \frac{b_{nm}}{4\pi} = 0 \end{array} \right. \quad (6)$$

Generally, one should possess the same number of variables and equations. In order to limit the higher order up to 5, we use a system composed of 35 equations. The main problem here is to find the roots which determine the position of the 35 magnetic rods.

#### IV. MEASURED FIELD DECOMPOSITION

We have to calculate the measured field in terms of Legendre expansion so as to identify with the opposite field created by shims and cancel parasitic  $A_{nm}, B_{nm}$ . Each component  $b_{mes}$  of a magnetic field is necessary unrolled as eq

$$b_{mes}(r, \theta, \phi) = \frac{1}{4\pi} \sum_{n=0}^{\infty} \sum_{m=0}^n (A_{nm} \cos(m\phi) + B_{nm} \sin(m\phi)) r^n P_{nm}(\cos \theta)$$

In order to respect the orthogonality of Legendre functions on a spherical surface only, it is necessary to take the points of measurement on a sphere. All points inside or outside this sphere contribute to loose the expansion accuracy. However, it is often mechanically easier to proceed with a rectangular mesh of points separated by a distance  $h$ . We propose to keep all points which are the nearest of the sphere [4] as shown in Fig.(1).

The algorithm presented in Appendix is suitable for the  $A_{nm}, B_{nm}$  calculations for 350 measured points. It calculates a eighth order expansion to avoid high-order harmonics aliasing.

#### V. SIMPLE GENERATION WITH TWO AND THREE MAGNETS

To illustrate the algorithm by a graphical method, we first determine the position of two magnets which generate a homogeneous field along the z-axis. Their first configuration is shown in Fig.(2) and the characteristics of the magnets are arbitrary given. As we are only interested in the axial  $B_z$  field, their position in  $\phi'$  becomes trivial. This study is instructive because we can transpose the two-dimensional into a more complicated example of n-dimensional case.

##### A. Aspect of the $a_{00}, a_{10}, a_{20}$ Curves.

These first coefficients of Eq.(5) are shown in Fig.(3). The  $a_{00} = \text{constant}$  curve is represented in two and three dimensions (two and three magnets), the axial coordinates are those of the magnets. One notices that the transposition is easy because the  $f(z_1, z_2) = \text{constant}$  curve is identical to the  $f(z_1, z_2, z_3 = 0) = \text{constant}$  curve. We can find the two-magnet curve from the cross section of a three-magnet curve. The  $a_{00} = 0$  curve is rather subtle as the x and y axes are asymptotic at infinity, there exists also a virtual curve when  $z_1 = z_2 = \infty$ . However, we are not interested in these remote solutions, and are

confined our study to  $\pm 20$  cm. We recall that throughout the text, we have normalized the dimension of the generator to  $r'=10$  cm. This is not absolutely restrictive because it is a matter of dimension ratio between  $r$  and  $r'$ , we assume that the magnets could displace from  $2r'$  to  $-2r'$ .

Fig.(4) represents the two  $a_{10} = 0$  and  $a_{20} = 0$  curves. It is up to us to find the intersection point of the simultaneous solution. The particularity of the first equation is that it is composed of a straight line ( $z_2 = -z_1$ ) and curves tangential to the  $a_{20}$  solution points. The multi-dimensional Newton-type algorithms fail here because the following vector solution is determined by the hyperplane intersection, the latter being tangential to curves at the current point. One can imagine therefore that a solution determined by two tangential curves cannot be found. This precise case, the solution is evident because the second curve is automatically intersected by a straight line. The plot of the dotted polyline represents the path followed during the search for solutions. One notes that the fourth segment is very close to the solution but it is then later eliminated. The second approach is realized by using the Singular Value Decomposition algorithm, as a hyperplane is removed if it is parallel to another. The solution is then found. Two Jacobian straight lines are identical, therefore the split up in singular value will suppress one of the lines and will continue under the form of a resolution in the least square sense. Nevertheless, if the initial vector fits into  $z_2 = -z_1$ , a solution will be found very rapidly, even with the Newton-Raphson method.

### *B. Choice of initial vectors*

The generation of a simple field implies that the Legendre coefficients are zero. We often find a straight line of the type  $z_1 \pm z_2 \pm \dots \pm z_n = 0$ . Even alone by themselves, certain equations comprise several straight lines, i.e.  $a_{31} = 0$ . It is particularly advisable to choose an initial vector the components of which are composed of the same absolute value chosen randomly and with a sign in accordance with the equation of this straight line. In this manner, the vector sticks to the plane, and is therefore less subject to the phenomenon of tangential curves. In physical terms, we can relate this to different symmetries, but mental effort becomes considerable when the number of orders to be corrected becomes large. It would be interesting then to review the various straight line equations and test the initial

vectors. A rough method consists in trying all the sign combinations, in the case of 35 equations, the total number of initial vectors is  $2^{34} = 17\,179\,869\,184$ . Nevertheless, these considerations are only valid in the case of coefficient cancellation. In the opposite case, the straight lines disappear as we can notice in Fig.(5). It does not exist therefore pure symmetry if the coefficient considered is not zero.

It seems difficult, however, to search for solutions that will cancel certain coefficients because the function is not finite everywhere. This is precisely at the solution points 1,2,3,and 4 of Fig.(4) that one of the functions is not derivable. Experiment has shown that it is simpler to correct a magnetic field where none of its coefficients is zero, than to generate a particular field profile the equation of which involves a priori many null terms. We have thus demonstrated the interest of eliminating one of the tangent planes by our algorithm. Due to boundary effect, we thus try not to approach too close to the solution so as to avoid an erroneous Jacobian calculation, as certain functions are not derivable on these points. It is therefore the approach of the solution in the least square sense, which eliminates this difficulty.

## VI. NUMERICAL INVERSION METHOD

In vector notation, we expand each function via the Taylor series. We only retain linear terms and equate this set to zero as in

$$F(\mathbf{x} + \delta\mathbf{x}) = F(\mathbf{x}) + J.\delta\mathbf{x} + O(\delta\mathbf{x}^2) = 0 \quad (7)$$

where  $x$  can be calculated with singular value decomposition (SVD).

$$\delta\mathbf{x} = \left[ \frac{\partial F}{\partial z} \right]^{-1} .z = V.[diag(1/w_i)].U^T.z \quad (8)$$

To correct static field defects, we use a bird-cage configuration composed of 35 permanent magnetic rods of 4mm diameter and 5mm long. Each rod is inserted in a glass tube and can slide along the  $z$  axis over 30cm. The cage radius is 10cm. After each field measurement, we compute and correct the position of these magnets. One of the behaviors of this kind of equation (Green Function) tends to eject these sources very far from their normal spatial position. All improperly placed sources can cause more errors than without sources. These practical considerations show that it is impossible to solve this

inverse problem by a classical linear inversion method. The inversion of Jacobian Matrix is rather subtle, the singular value decomposition shows that the ratio of the largest diagonal matrix element to the smallest is equal to 10 20. The following is a useful procedure to find roots of Eq.(5). At the start, the initial magnet positions are chosen randomly in the whole interval determined by the length of the bird-cage( $\pm 15\text{cm}$  in our case). A minimum threshold value  $w_i = 0.01$  is defined so that, of the 35 equations, only half will be incorporated in the set. After 1000 iterations, we retain the intermediate solution which generates the least error, the latter being the sum of residual errors of each equation of Eq.(5). The second step is to divide by 10 the minimum threshold so that 60% of the equations are incorporated and the random-value interval is centered around the previous solution( $\pm 1\text{cm}$ ). We keep this solution and divide again by 100 the initial threshold. However, for the following steps, the relative interval remains unchanged and is equal to  $\pm 1\text{cm}$ . The procedure is stopped when the precision of the roots is sufficient, the threshold is generally equal to  $10^{-6}$ . The calculation time is that of 4000 iterations of SVD of a matrix with 35x35 elements. Using a 10 MFlops computer, the elapsed time is 24 minutes.

## VII. STATIC CORRECTED FIELD RESULTS

Our practical case is to improve the homogeneity of a static magnetic field. Using the present bird-cage configuration, the inhomogeneity of the static field Fig.(6) is improved by a factor of 100 as illustrated in Fig.(7). Both figures show only the differential values of the field intensity. Actually the final field intensity is of the order of one Gauss higher, which is due to the elementary fields produced by the permanent magnetic rods. Also, the final position of these rods are within a distance of less than 12cm from the center of the z-axis.

## VIII. CONCLUSION

Some restrictions may appear, among which, the field strength, while others are dissimulated. The software program shows also those impossible cases. These studies are very interesting because we can change our initial configuration. Some parts of the Legendre system are crucial. For example, in the case of a uniform field generation represented by

$A_{00}$ , the most important coefficient is  $A_{20} = -r^2/2 + z^2$  which represents the difference between the curvature along  $z$  and the  $xy$  curvature.  $A_{20}$  is hard to obtain in the case of plane or cylindrical geometry, because sources should be uniformly distributed all over the volume of interest to have suitable curvature at the origin. Bearing in mind that a uniform field exists inside a sphere. In the case of linear field ( $x$  gradient  $A_{11}$ ),  $A_{31} = 3x(-r^2/2 + 2z^2)$  is one of the most important coefficients. It's yet more difficult to have a good precision gradient than a uniform field because the  $z^2$  coefficient renders  $A_{31}$  very difficult to annul.

## IX. APPENDIX

This algorithm can be used to calculate the  $A_{nm}$ ,  $B_{nm}$  of a measured field. The  $lgndr(n,m,x)$  numerical function should be found in [2].

COEFFICIENTS()

```

1  nmax ← 8
2  nbvara ← 45
3  nbvarb ← 36
4  nbvar ← nbvara + nbvarb
5  nbpoints ← 350
6  for i ← 1 to nbpoints
7    do x[i] ← ?
8      y[i] ← ?
9      z[i] ← ?
10     field[i] ← ?
11
12  for k ← 1 to nbvar
13    do bet[k] ← 0.
14      for l ← 1 to nbvar
15        do u[k][l] ← 0.
16
17  for i ← 1 to nbpoints
```



```

18  do  $r \leftarrow \sqrt{x[i]^2 + y[i]^2 + z[i]^2}$ 
19    for  $k \leftarrow 1$  to  $nbvara$ 
20      do  $n, m \leftarrow \text{DETANM}(k)$ 
21         $a[k] \leftarrow (-1)^m r^n \text{lgndr}(n, m, z[i]/r) \cos(m \arctan(y[i], x[i]))$ 
22         $bet[k] \leftarrow bet[k] + field[i] \times a[k]$ 
23
24    for  $k \leftarrow 1$  to  $nbvarb$ 
25      do  $n, m \leftarrow \text{DETBNM}(k)$ 
26         $a[k + nbvara] \leftarrow (-1)^m r^n \text{lgndr}(n, m, z[i]/r) \sin(m \arctan(y[i], x[i]))$ 
27         $bet[k + nbvara] \leftarrow bet[k + nbvara] + field[i] \times a[k + nbvara]$ 
28
29    for  $k \leftarrow 1$  to  $nbvar$ 
30      do for  $l \leftarrow 1$  to  $nbvar$ 
31        do  $u[k][l] \leftarrow u[k][l] + a[k] \times a[l]$ 
32
33
34
35  for  $l \leftarrow 1$  to  $nbvar$ 
36    do  $sol[l] \leftarrow \sum_k u^{-1}[k][l] \times bet[k]$ 
37

```

DETANM( $i$ )

```

1   $indent \leftarrow 0$ 
2  for  $n \leftarrow 0$  to  $nmax$ 
3    do for  $m \leftarrow 0$  to  $n$ 
4      do  $indent \leftarrow indent + 1$ 
5        if  $indent = i$ 
6          then return  $n, m$ 
7
8

```

9 **error** “ $i \notin [1, nbvara]$ ”

DETBNM( $i$ )

1  $indent \leftarrow 0$

2 **for**  $n \leftarrow 1$  **to**  $nmax$

3     **do for**  $m \leftarrow 1$  **to**  $n$

4         **do**  $indent \leftarrow indent + 1$

5             **if**  $indent = i$

6                 **then return**  $n, m$

7

8

9 **error** “ $i \notin [1, nbvarb]$ ”

## REFERENCES

- [1] D. I. Hoult F. Romeo. Magnet field profiling: Analysis and correcting coil design. *Magnetic Resonance in Medicine*, 1:44–65, 1984.
- [2] Press Vetterling Teukolsky Flannery. *Numerical Recipes in C*. Cambridge University Press, 1992.
- [3] H. Feshbach P. M. Morse. *Methods of Theoretical Physics*. Mc Graw-Hill Book Compagny, 1953.
- [4] P. N. Swarztrauber. On the spectral approximation of discrete scalar and vector functions on the sphere. *SIAM J. Numer. Anal.*, 16, December 1979.
- [5] R. Vadovic. Magnetic field correction using magnetized shims. *IEEE Transactions On Magnetics*, 25(4):3133–3139, 1989.

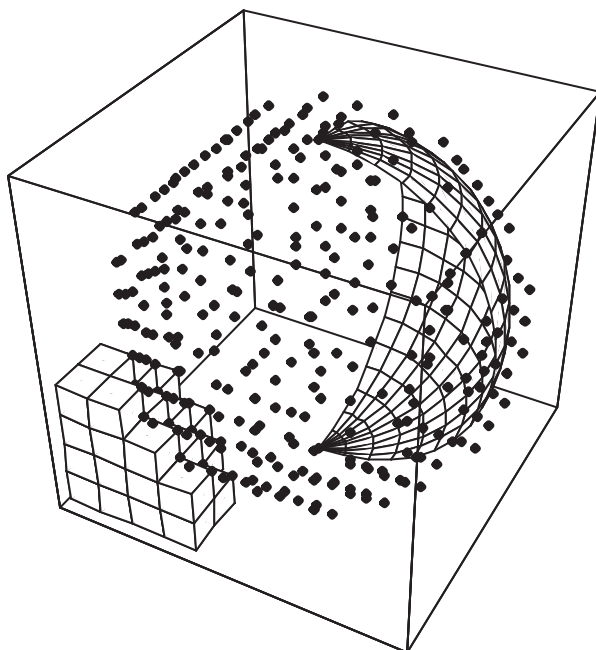


Fig. 1. Field measurement on a sphere of radius  $R \pm h$ .

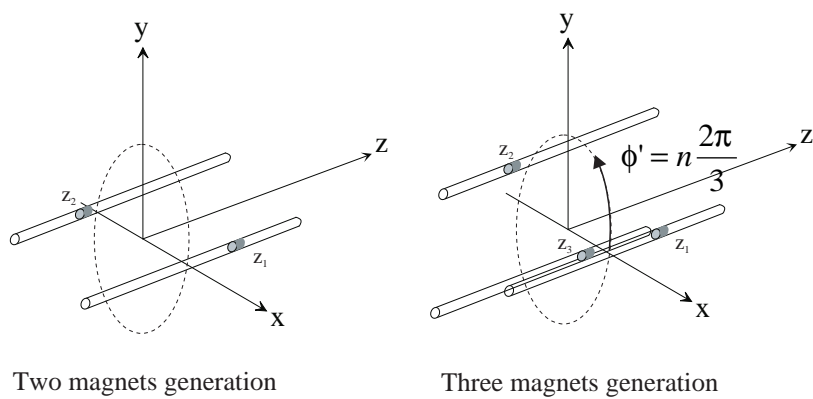


Fig. 2. Some simple configurations.

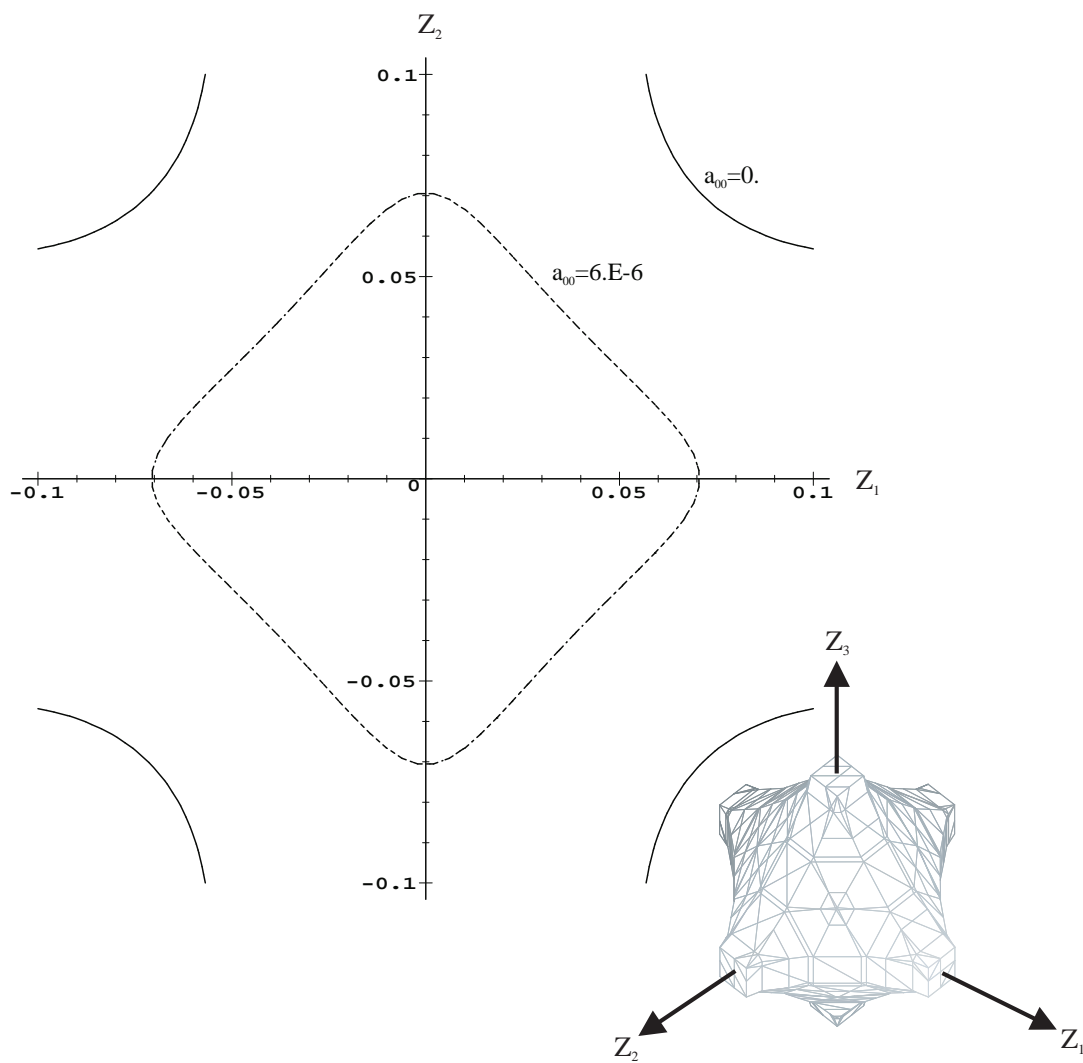


Fig. 3.  $a_{00}$  for two and three magnets. The axes represent the positions of the magnets along the sliding rods.

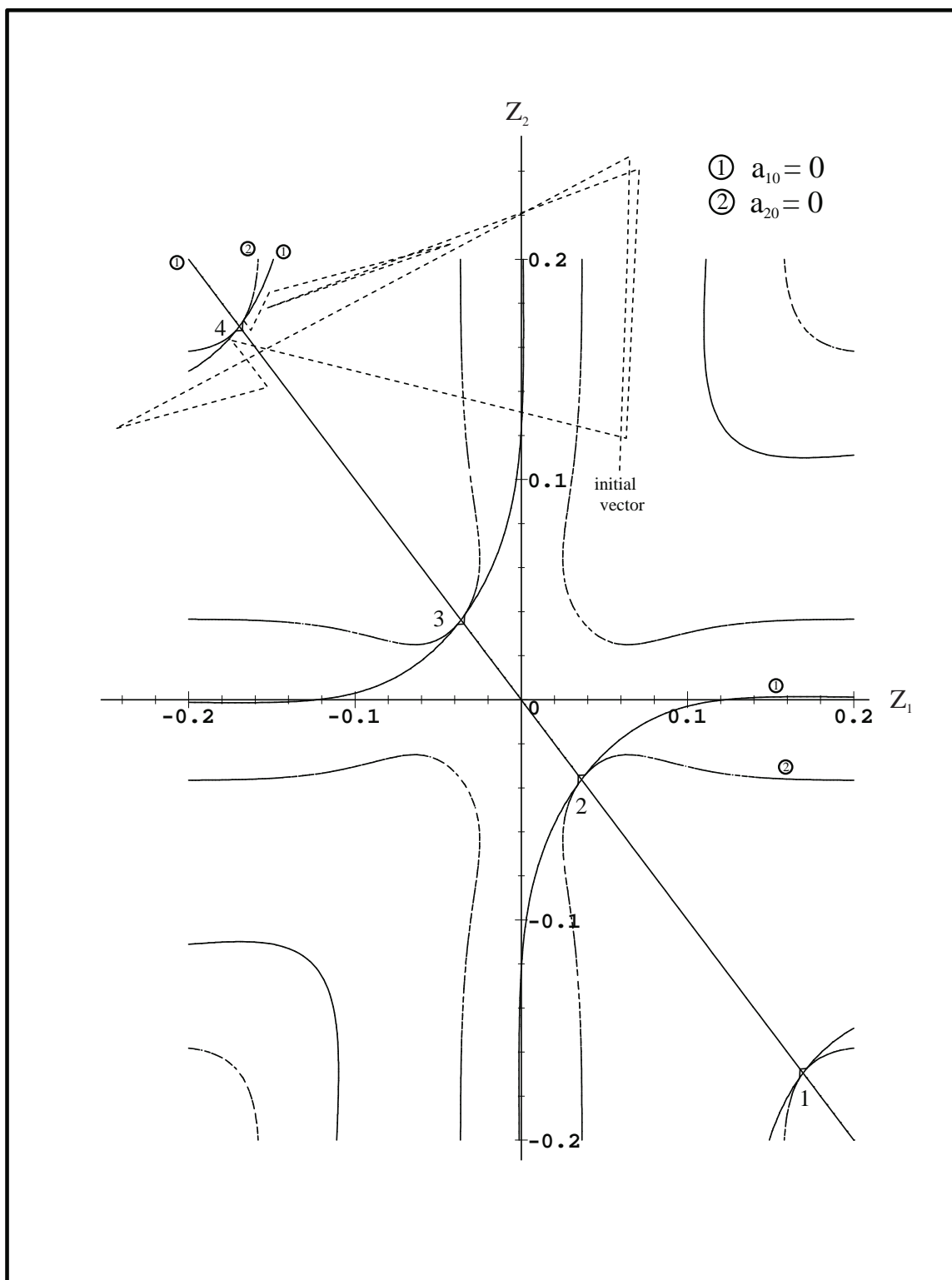


Fig. 4. Search for solution by the Newton algorithm for the first four segments. Upon failure, the final approach is performed by elimination of tangent planes.

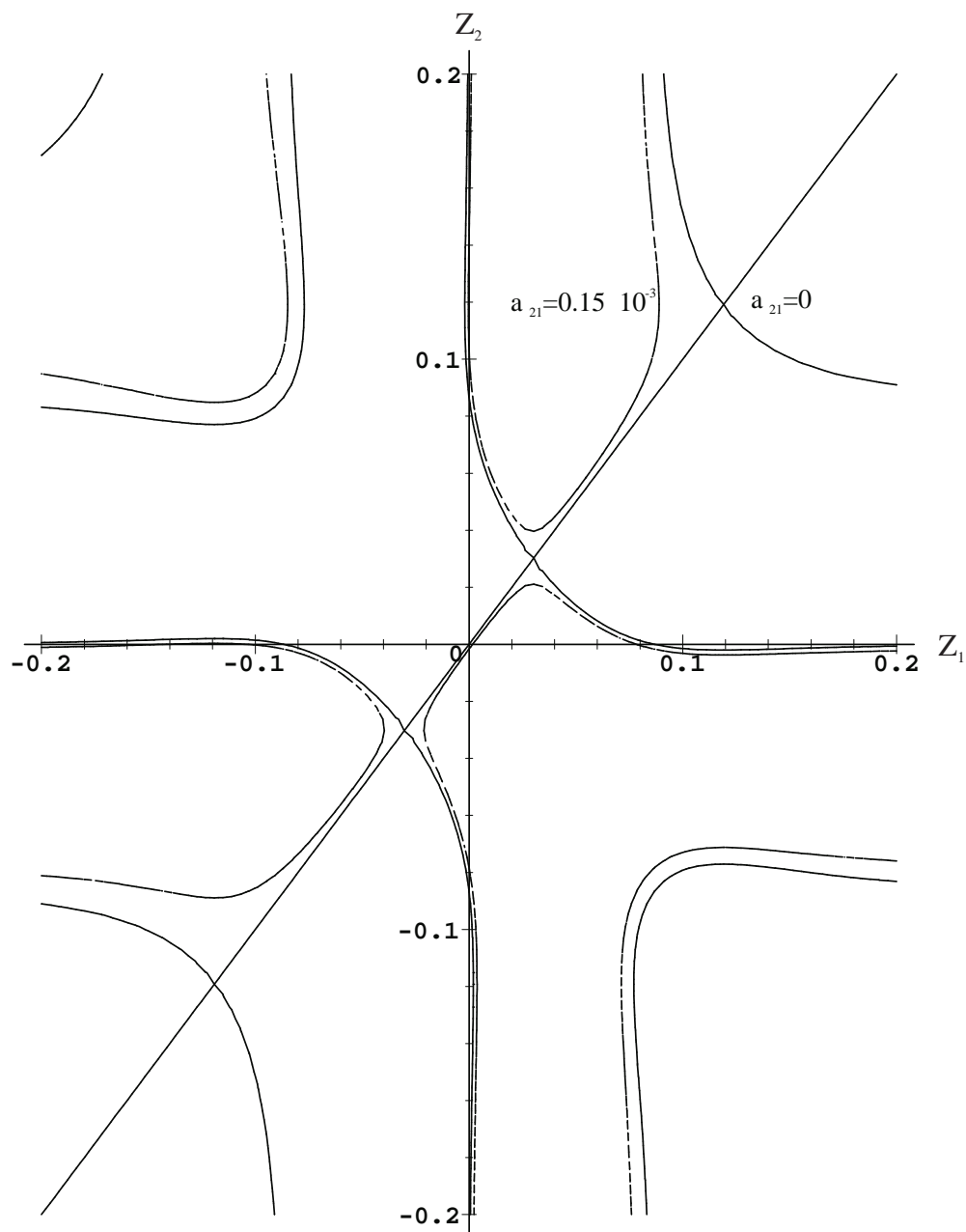


Fig. 5. Symmetries exist only in the case when the coefficients are zero.

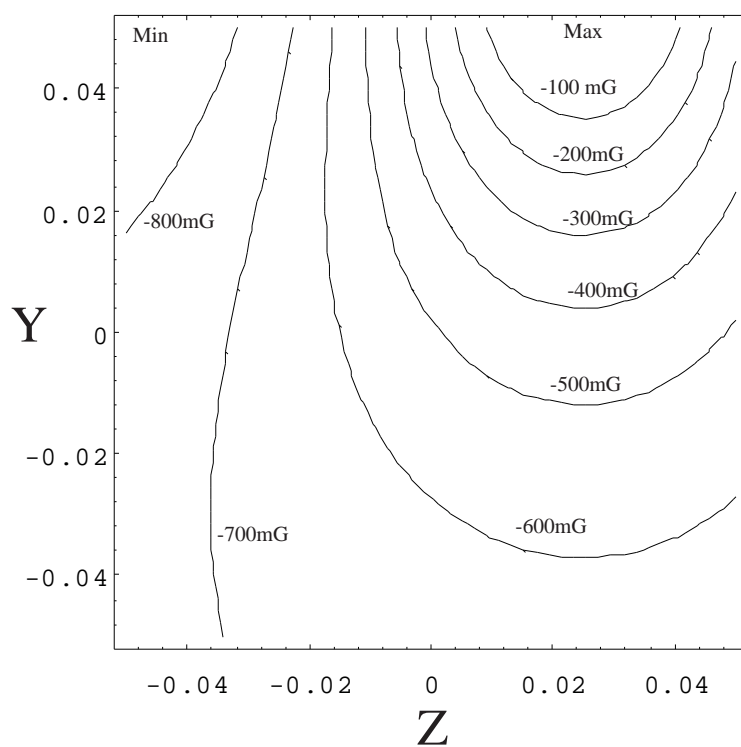


Fig. 6. Isovalue plot of the initial main field

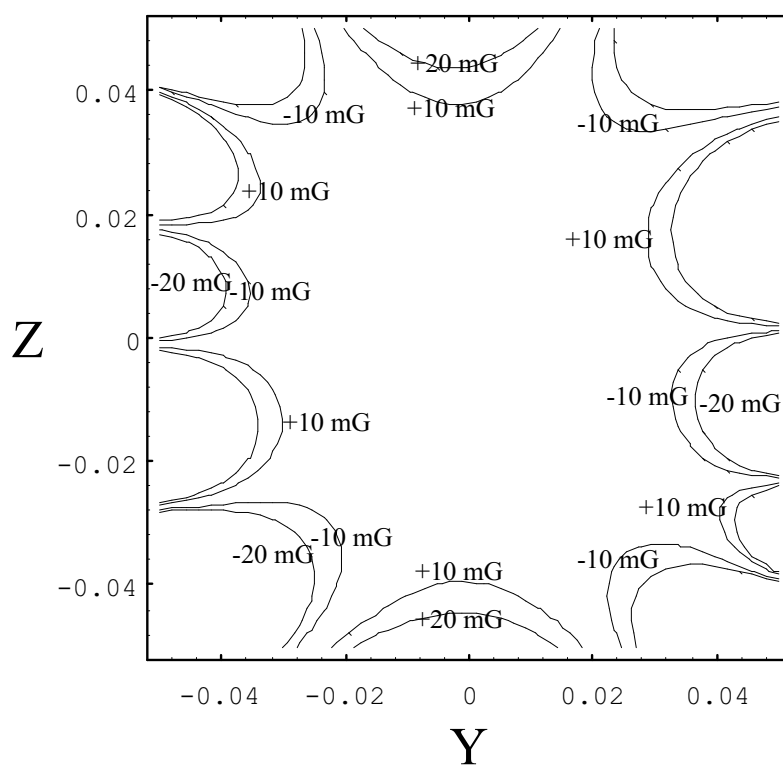


Fig. 7. Isovalue plot of the corrected field